Surface Coatings- and Light- Controlled Oxygen Doping of Carbon Nanotubes

Fjorela Xhyliu, Geyou Ao *

Department of Chemical and Biomedical Engineering, Washkewicz College of Engineering, Cleveland State University, 2121 Euclid Avenue, Cleveland, OH 44115, USA

Corresponding Author

*Email address: g.ao@csuohio.edu

ABSTRACT

Tuning optical properties of single-wall carbon nanotubes (SWCNTs) *via* oxygen doping has been a simple and effective approach to create fluorescent quantum emitters. We performed oxygen doping of SWCNTs in water utilizing chirality-pure (6,5) enantiomers with different surface coatings of DNA and surfactants by ultraviolet (UV) light irradiation. We found the reaction to be primarily dependent on the wavelength of UV light and the specific coating material on the nanotube surface. Particularly, DNA coatings react more readily with reactive oxygen species that is photochemically produced at a short wavelength UV light than SWCNTs, preventing oxygen doping of nanotubes to occur. The surface coverage of SWCNTs created by coating materials plays a weaker role on controlling the reaction efficiency of oxygen doping. This is demonstrated clearly by the lack of oxygen doping for two (6,5) enantiomers wrapped by DNA with drastically different surface coverage. These findings reveal important mechanisms of oxygen doping of

SWCNTs, providing methods of controlling optical properties of nanotubes for developing unique applications.

INTRODUCTION

Surface chemistry of carbon nanotubes offers vast possibilities for tuning the electronic structures of nanotubes and property enhancement, therefore enabling applications including biochemical sensing and imaging,[1,2] optoelectronic devices,[3] and photonics.[3–5] Covalent modification of semiconducting single-wall carbon nanotubes (SWCNTs) is of growing interest due to its robustness and versatility in creating highly emissive deep trap states on the sidewall of SWCNTs. Specifically, covalently-doped SWCNTs have been achieved through various routes such as oxygen doping *via* bleach[2] or ozone treatment,[6–9] as well as reactions with diazonium salts[10–12] and other functional groups.[13–16] While oxygen doping of SWCNTs can lead to a stable, ether-type oxygen adduct that can maintain the sp^2 carbon hybridization,[5,8] diazonium and other doping approaches create sp^3 defects on the sp^2 carbon lattice of SWCNTs.[10,11] Furthermore, chemical adducts that are introduced covalently are shown to yield brighter photoluminescence (PL) with longer exciton lifetimes[17] at a new, red-shifted wavelength in the near-infrared (NIR) region due to the trapping of mobile excitons at the synthetic dopant sites.[5,18] This makes functionalized SWCNTs more desirable as NIR fluorescent probes for biomedical imaging,[2,6] in addition to providing a source for single photon emission[4,18] and other optoelectronic applications.

In addition to the chemical nature of doping molecules, environmental effects[8] such as solvents and coating materials on the surface of SWCNTs, as well as the light source[2,11] utilized for nanotube chemistry can affect the efficiency of reactions and the resulting deep trap emission features. Different dielectric environments experienced by chemically introduced sites due to

variations in the surrounding solvent or the surface coverage along the length of nanotube created by coating materials can lead to a large inhomogeneous broadening of deep trap emission.[8,19,20] Solvent plays an important role during the reaction, affecting the lifetime of the defect-state PL.[20] Various solvents, such as water,[20,21] deuterium oxide (D_2O),[10,11] and organic solvents[12,20] have been utilized for SWCNT functionalization. Furthermore, surface coatings of SWCNTs play a significant role during the covalent modification reactions. Depending on the surfactant identity and concentration, the reaction can either be facilitated or inhibited, particularly for the covalent oxygen doping of SWCNTs.[2,22] Ghosh et al. were the first to observe the oxygen doping effect on SWCNTs that creates strong NIR emission with visible light and ozone treatments of nanotubes.[6] Since then, oxygen-doped SWCNTs have been produced *via* various routes at varying reaction time periods (from seconds to hours), including ozonolysis of air-suspended[7] and surfactant-dispersed SWCNTs in a solvent[6,8] under light exposure, as well as a solid state doping approach utilizing SWCNT matrices coated with an oxide thin film.[18,22]

Here, we demonstrated that the oxygen doping of pure-chirality (6,5) SWCNTs in deionized (DI) water is a readily occurring reaction when exposed simply to a short wavelength ultraviolet (UV) light (i.e., 254 nm) without adding extra chemicals and the reaction is strongly dependent on the specific coating material (i.e., DNA and different surfactants) on the SWCNT surface. The surface coverage of SWCNTs created by coating materials was found to play a weaker role in the oxygen doping reaction. Specifically, we purified a pair of (±) (6,5) enantiomers using the recognition single-stranded DNA sequence TTA TAT TAT ATT in a polymer aqueous two-phase system.[23] Subsequently, DNA coatings of purified (6,5) tubes were displaced by surfactants of various binding affinities to SWCNTs including sodium dodecylbenzene sulfonate (SDBS), sodium dodecyl sulfate (SDS), sodium cholate (SC), and sodium deoxycholate (SDC).

Particularly, SDC is known to interact with SWCNTs much stronger than other surfactants due to its rigid, steroid-ring structure that assists the formation of a homogenous, thick bound layer of surfactant around SWCNTs.[24–26] The set of DNA- and surfactant-wrapped (6,5) tubes in water were exposed to UV light to study the formation of fluorescent quantum defects *via* oxygen doping. We have performed a minimum of three repeats of each oxygen doping reaction and presented representative spectroscopy findings here. Additional data can be found in the Supporting Information.

EXPERIMENTAL SECTION

Polymer Aqueous Two-Phase Separation of (6,5) Enantiomers. Aqueous dispersions of DNA-wrapped SWCNTs (i.e., 1 mg/mL SWCNT – 2 mg/mL DNA) and pure-chirality (6,5) enantiomers were prepared according to our previously published procedure.[23,27] Briefly, CoMoCAT SWCNT powder (SG65i-L39, CHASM Advanced Materials) was dispersed in a total volume of 1 mL aqueous solutions of recognition DNA sequence TTA TAT TAT ATT (Integrated DNA Technologies) containing 0.1 mol/L NaCl by probe tip sonication (model VCX 130, Sonics and Materials, Inc.) in an ice bath for 2 hours at a power level of 8 W. Supernatant dispersions were collected after 90 min centrifugation at 17,000 g for SWCNT purification. A pair of (6,5) enantiomers were separated in a polymer aqueous two-phase (ATP) system containing 7.76 mass% poly(ethylene glycol) (6 kDa)/15.0 mass% polyacrylamide (10 kDa) (PEG/PAM).[23] Specifically, (−) (6,5) enantiomer was isolated in the PEG-rich top phase and (+) (6,5) enantiomer was separated in the PAM-rich bottom phase. Here, the plus or minus sign of (6,5) species is assigned according to the signs of the circular dichroism values at the E_{22} position of (6,5) near 573 nm. The (6,5)

SWCNTs have the enantiomeric excess of > 90% for each handedness tube based on our prior report.[23] Details of SWCNT separation by polymer ATP method can be found in prior work.[23]

After ATP separation of DNA-SWCNTs, polymers were removed according to the SWCNT precipitation method reported previously.[23,27,28] Briefly, a final concentration of 1.0 mol/L sodium thiocyanate (NaSCN, Sigma-Aldrich) was added to purified (6,5) SWCNT species in polymer phases, and the sample was incubated overnight at 4 °C. Adding the corresponding DNA recognition sequence at 100 μg/mL during the incubation stage is recommended to prevent nanotube aggregation. Then, the mixture was centrifuged at 17,000 g for 30 min to remove the solvent and the purified (6,5) SWCNT pellet was resuspended in deionized (DI) water by bath sonication at room temperature for 30 min. DNA sequence TTA TAT TAT ATT at a final concentration of 100 μg/mL was added to purified (6,5) enantiomers to improve the dispersion stability for a long-term storage.

Displacing DNA Coatings of (6,5) Tubes by Surfactants. Stock solutions of surfactants in DI water including 10 mass% sodium dodecylbenzene sulfonate (SDBS) (Sigma-Aldrich), 10 mass% sodium cholate (SC) (≥99% BioXtra), 10 mass% sodium dodecyl sulfate (SDS) (≥99% BioXtra), and 10 mass% sodium deoxycholate (SDC) (≥98 % BioXtra) were prepared for DNA/surfactant exchange reaction of purified (6,5) enantiomers. For the surfactant exchange procedure, stock purified DNA-(6,5) sample was mixed with various surfactants at a final concentration of 1 mass %. Mixtures were incubated in an oven at 40 °C for 10 minutes to allow for surfactant exchange, followed by 10 min bath sonication at room temperature. (6,5) tubes were then diluted in DI water to obtain 150 μL sample with an absorbance value of 0.1 ± 0.02 at the E_{11} peak wavelength near 985-992 nm, which corresponds to approximately 0.65 μg/mL concentration of SWCNTs,[29] for the subsequent oxygen doping reaction. The corresponding concentrations of

coating materials are provided in Table S1. We utilized absorption and fluorescence spectroscopy of SWCNTs to monitor the DNA/surfactant exchange reaction according to our previous work (Figures S1, S2 and Tables S1, S2).[30] The final concentrations of surfactants in (6,5) tubes utilized for oxygen doping experiments are lower than the critical micelle concentration (CMC) values (Table S1).

Oxygen Doping Reaction of (6,5) Tubes. For oxygen doping reactions of (6,5) tubes with different coatings (i.e., DNA and various surfactants), SWCNT samples were left exposed to ambient air for 30 minutes before ultraviolet (UV) light (3UV Lamp, cat# 95034, Thermo Scientific) exposure. Specifically, (6,5) tubes were exposed to 254 nm and 365 nm wavelengths UV light at a power density of ≈13 mW/cm^2 for the desired time period. (6,5) samples were kept in an ice bath when exposing to UV light for the desired time to avoid overheating of nanotube samples. Additionally, oxygen removal of (6,5) samples was performed at room temperature to investigate the effect of dissolved oxygen amount on the oxygen doping of SWCNTs. Cuvette containing SWCNT sample was inserted with a needle connected to a vacuum pump (8907, Welch). Samples were left under vacuum for a few seconds up to a minute until bubbles were no longer formed. Then, the vacuum needle was switched for the needle connected to an argon (Ar) gas tank in order to purge the sample with Ar and replace remaining air in the cuvette. This process took only 1-2 seconds due to the small volume capacity of the cuvette. The process of vacuum to purging with Ar was repeated for at least three times to ensure air bubbles were no longer formed.

Optical Spectroscopy Characterization. Optical spectroscopy characterization including vis-near infrared (NIR) absorbance, NIR fluorescence and Raman spectra measurements were performed on a NS3 Nanospectralyzer (Applied NanoFluorescence, LLC) using a 10 mm path length quartz cuvette. Due to extremely dilute concentration of SWCNTs in samples, the D peak

near 1320 cm^{-1} for oxygen-doped nanotubes in Raman spectra was not obvious. For DNA/surfactant exchange, DNA coating displacement by a surfactant was characterized by absorption and fluorescence spectral changes of the E_{11} peak of (6,5) species (Figure S1 and S2, Table S2). Specifically, Table S2 summarizes the fluorescence spectral changes including the solvatochromic shifts (i.e., spectra shifts) and changes in emission intensity at the E_{11} peak wavelength of (6,5) tubes. Fluorescence spectral changes of nanotube are caused by variations in the environmental dielectric constant due to the DNA coating displacement by surfactants. For oxygen doping experiments, optical spectra of (6,5) samples were measured before and after the oxygen removal process as well as before and after UV light exposure. For peak fitting of oxygen-doped SWCNTs, the E_{11} and E_{11}^{-} emission peaks were fitted with Voigt profiles using Origin Pro 2019b v2, and the ratio of the integrated peak areas were plotted to obtain the relative doping degree percentage.

RESULTS AND DISCUSSION

As a quasi-one-dimensional (1D) nanomaterial, SWCNTs are of high interest for covalent modification because all atoms are exposed to the surface, providing vast potential for introducing chemically stable sites such as oxygen adducts. These dopant sites can effectively trap the intrinsic 1D mobile excitons in SWCNTs to zero-dimensional (0D) localized states, therefore creating a 0D-1D hybrid low-dimensional system with tunable optical properties.[5,31,32] It has been shown that SWCNTs can react with dissolved oxygen at ambient condition *via* a reversible redox reaction due to charge transfer with adsorbed oxygen species, resulting in the quenching of nanotube fluorescence at the pristine E_{11} peak.[29,33] However, it is also possible to produce reactive oxygen species (ROS) *via* a photochemical process under high energy, short wavelength UV

irradiation,[34,35] and the highly reactive oxidant can irreversibly react with SWCNTs through forming covalent C-O-C bonds of ether or epoxide adducts on the nanotube.[8] These oxygen adducts that are introduced covalently on the surface of SWCNTs create a new E_{11}^{-} peak that fluoresces at a longer wavelength. Here, when SDBS-coated (–) (6,5) species were exposed to 254 nm wavelength UV light for 50 minutes, we observed a new, red-shifted emission peak (E_{11}^{-}) at 1131 nm accompanied by a decrease in the emission intensity of the pristine E_{11} peak of (–) (6,5) at 986 nm (Figure 1a). The corresponding energy separation ($\Delta E = E_{11} - E_{11}^{-}$) of the SDBS-(–) (6,5) sample after UV (254 nm) exposure yields 160 meV, indicating the formation of a stable, ether-type oxygen adduct with sp^2-hybridized carbon atoms.[8] The observed E_{11}^{-} emission wavelength is similar to that of oxygen-doped (6,5) samples obtained previously by ozone or bleach treatment.[2,6] The corresponding absorption spectrum of oxygen-doped (–) (6,5) showed decreases in absorbances values at both E_{11} (988 nm) and E_{22} (572 nm) optical transition peaks by 29.1% and 17.5%, respectively, which originate from the perturbation in the π-electron system of nanotubes from covalent functionalization (Figure 1b).[2]

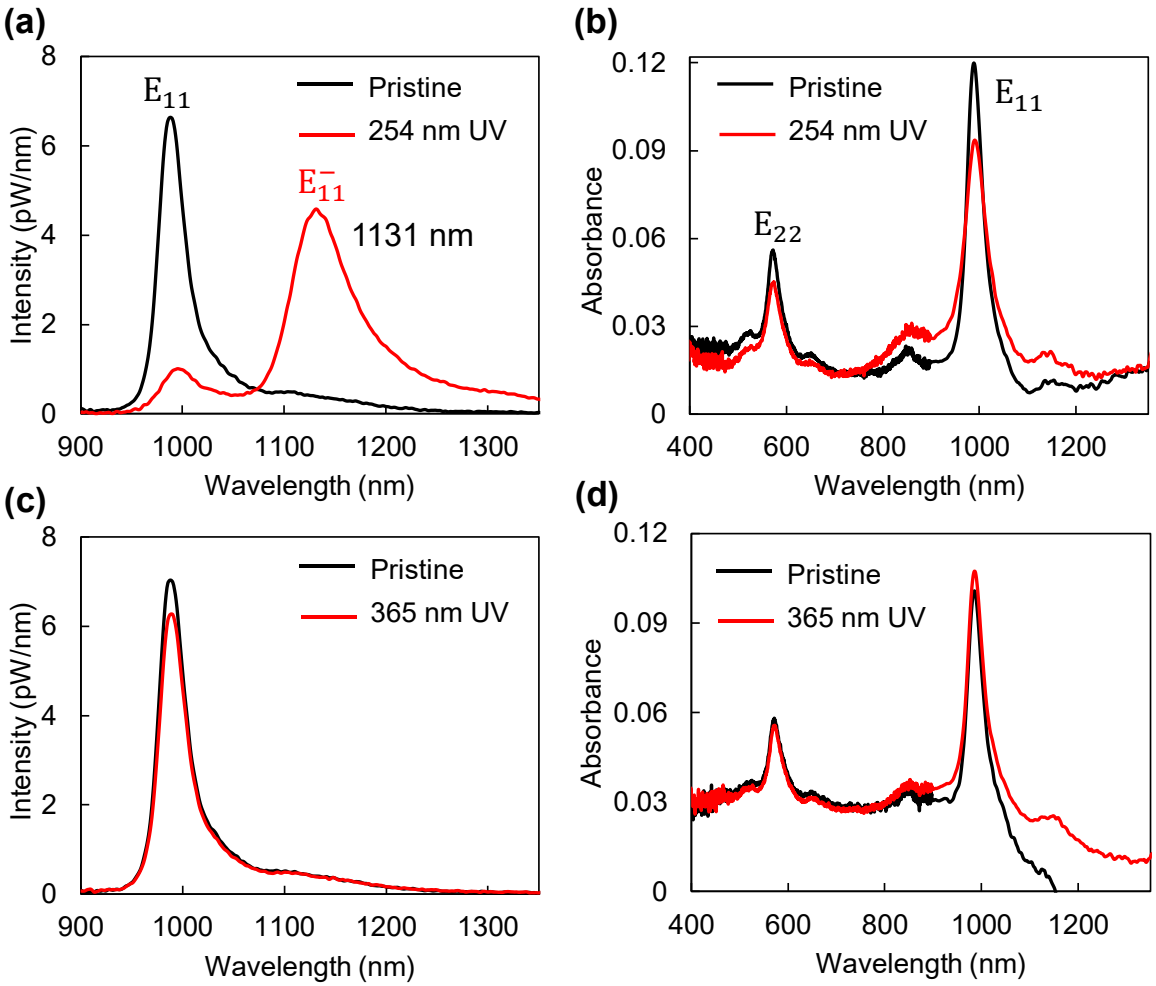

Figure 1. Oxygen doping of SDBS-coated (–) (6,5) complex with UV light illumination. **(**a) Fluorescence and (b) absorbance spectra of (–) (6,5) before (i.e., pristine) and after being exposed to 254 nm UV light for 50 minutes. In comparison, (c) fluorescence and (d) absorbance spectra of (–) (6,5) exposed to long wavelength UV light (365 nm) for 50 minutes did not show the E_{11}^- optical features of doped SWCNTs.

In comparison, no evidence of a new E_{11}^- emission peak was found when the SDBS-(–) (6,5) sample was exposed to a 365 nm wavelength UV light for 50 minutes (Figure 1c). The slight decrease (i.e., 9 %) in the pristine E_{11} emission intensity is likely caused by a minor change in the local dielectric environment surrounding nanotubes due to variation in surfactant coating structure with UV irradiation (Figure 1c). The corresponding absorption spectrum remains essentially unchanged (Figure 1d). This could be due to the lower energy of 365 nm UV light being

insufficient to produce ROS, as the UV absorption of molecular oxygen at various states occurs below 300 nm.[36] Additionally, UV light induced excitation of semiconducting (6,5) tubes may promote the energy exchange between the excited state SWCNTs and some oxygen molecules that may have been adsorbed on the nanotube surface, possibly facilitating the oxygen doping reaction.[11,37] The proposed photochemical reaction of SDBS-SWCNTs in the presence of dissolved oxygen and short wavelength UV light is illustrated in Scheme 1. Particularly, UV light irradiation of aqueous dispersions of SWCNT samples likely leads to ROS generation *via* photoactivation of dissolved oxygen, and ROS further reacts with nanotubes to create fluorescent quantum defects. Although the mechanism of ROS generation may be rationalized by future studies, the phenomenon of defect-state E_{11}^{-} peak formation with a separation energy of 160 meV for SDBS-SWCNTs suggests ether-type oxygen doping of nanotubes by highly reactive oxidant. Additionally, we performed control experiments to further determine the role of dissolved oxygen on the covalent-doping of SDBS-(–) (6,5) in water by oxygen removal through a combination of vacuum and purging samples with argon. The treatment was effective to a certain extent, as evidenced by the increase in pristine nanotube PL after the oxygen removal process (Figure S3).[33] The resulting sample was irradiated with 254 nm UV light. We observed the appearance of E_{11}^{-} fluorescence peak at 1123 nm in SDBS-(–) (6,5) complex after oxygen removal treatment, indicating nanotube reaction due to the remaining small amount of dissolved oxygen in water. However, the emission intensity ratio I_{11}^{-}/I_{11} (i.e., I_{11}^{-} corresponds to the intensity of E_{11}^{-} peak, and I_{11} is intensity at the pristine E_{11} peak before reaction) of 0.38 for SDBS-(–) (6,5) with oxygen removal is lower than that of untreated sample with $I_{11}^{-}/I_{11} \approx 0.63$ (Table S3). This indicates that a sufficient amount of dissolved oxygen is needed to facilitate the UV light induced oxygen doping of SWCNTs.

Scheme 1. Oxygen doping of SWCNTs by UV light irradiation in water.

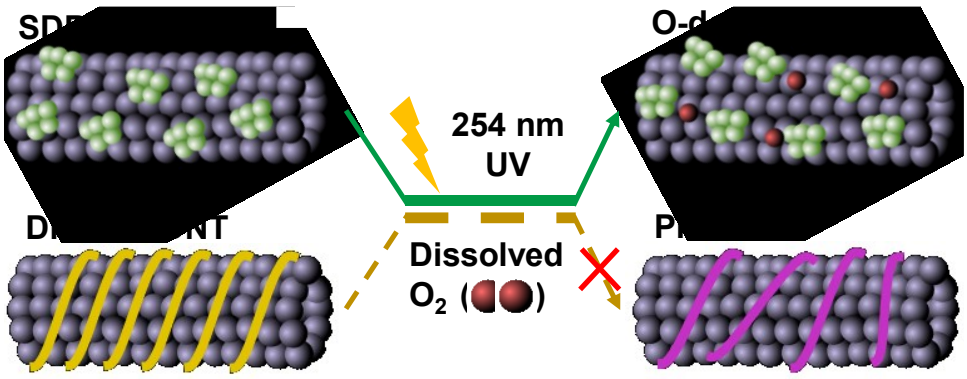

Figure 2 shows the reactivity of oxygen doping of SDBS-(–) (6,5) samples by plotting the growth of the dopant-induced emission intensity at E_{11}^{-} peak and the decrease of the pristine E_{11} emission intensity, respectively, as a function of UV (254 nm) exposure time. The formation of defect-state E_{11}^{-} peak occurred within 20 minutes of UV light irradiation. Particularly, the E_{11}^{-} emission intensity increased initially with UV exposure time and reached a maximum near 50 minutes. This is followed by a continuous decrease in intensity with longer irradiation time. Additionally, we observed an energy separation of up to $\Delta E \approx 176$ meV and broadening of E_{11}^{-} emission peak when UV irradiation was longer than 50 minutes (Figure S4). These observations indicate that the optimum UV exposure time for forming stable, ether adducts on SDBS-(–) (6,5) samples under our experimental condition is around 50 minutes and extended UV light irradiation will result in the creation of excess defect sites along the nanotube surface.[8] In comparison, the pristine E_{11} emission intensity decreases by 40 % within 20 minutes of UV irradiation and decays monotonically. The corresponding absorbance values at E_{11} remain relatively stable up to an hour of UV light exposure and decrease slightly for the duration of a 3 hour experiment, indicating that SWCNTs remain relatively stable during the photochemical reaction process (Figure S5). In the

following experiments, we compared the effect of coatings materials on the oxygen doping of SWCNTs using 254 nm UV light with 50 minutes exposure time.

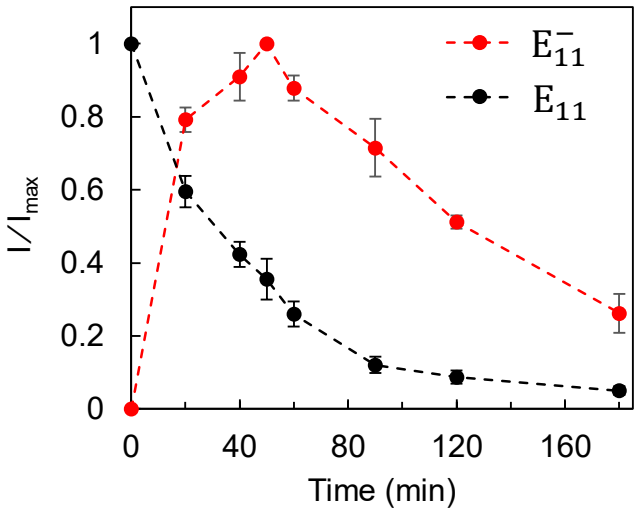

Figure 2. Normalized emission intensities of defect-state E_{11}^{-} peak near 1131 nm and pristine E_{11} peak at 986 nm for SDBS-(–) (6,5) complex as a function of UV (254 nm) irradiation time. I denotes the emission intensity of E_{11} and E_{11}^{-}, respectively, at varying time periods. I_{max} denotes the maximum emission intensity of E_{11} (before reaction) and E_{11}^{-} (after reaction), respectively. Dashed lines are provided as a guide for the eye. The error bars were obtained from the standard deviation of three repeats.

We performed UV irradiation of (–) (6,5) tubes wrapped by different coating molecules including the recognition DNA sequence and three additional surfactants with varying ability to stabilize SWCNTs in water (Figure 3). Among the (–) (6,5) samples that we have investigated, the formation of a defect-state E_{11}^{-} emission peak was not observed for nanotubes coated by DNA and SDC (Figure 3a,b). It has been shown previously that oxygen doping of SWCNTs is highly dependent on the surfactant coating structures on the surface of nanotubes.[2,22] Particularly, SDC is known to interact with SWCNT strongly and form a compact, uniform coating layer around the SWNCTs which tends to shield the SWCNT surface from interacting with reactive dopant

species.[22,26] The compact coating structure of SDC is likely inhibiting the access of reactive dopant species to the nanotube surface, as evidenced by the pristine E_{11} emission remaining essentially unchanged with 254 nm UV irradiation (Figure 3b). On the other hand, we observed ≈ 47 % decrease in the pristine E_{11} emission intensity after UV exposure for DNA-(–) (6,5), while a new red-shifted E_{11}^{-} peak did not form. This is particularly interesting because an ordered DNA wrapping structure is known to form around a specific SWCNT species as a result of a DNA recognition sequence based sorting of SWCNTs, exposing a certain degree of bare SWCNT surfaces that do not interact with DNA.[38,39] The exposed SWCNT surface is likely to interact with reactive species in the surrounding environment.

We speculate that DNA coatings around SWCNTs protect nanotubes from highly reactive oxidant in this scenario due to its unique physicochemical property. First, it is known that ROS causes oxidative DNA damage in a site-specific manner, and degradation of thymine residues has been observed in adenine/thymine (A/T) rich regions during ozonolysis.[40–42] The recognition sequence of (6,5) enantiomers is composed of A/T nucleobases, which may react with ROS more readily than SWCNTs. Second, DNA coatings on the nanotube effectively absorb 254 nm UV light, which is resonant with the DNA π-π^* absorption band at ≈ 240-285 nm, therefore attenuating the UV radiation effect on SWCNTs through energy transfer.[43] The resulting charge transfer from the UV photoexcited nucleobases to the SWCNT is likely the reason for the quenching of nanotube PL observed in Figure 3a. The phenomenon of strong quenching of the nanotube PL has been observed previously for DNA-SWCNT samples as well when the UV excitation is in resonant with the DNA absorption.[44] Third, recent work has shown that the tightly bound DNA wrapping around a SWCNT could lead to a higher surface coverage than that of weak surfactants due to the strong interactions between the nucleobases and the surface of SWCNTs

resulting from a combination of van der Waals, hydrophobic, and Coulomb forces.[39,45] The high surface coverage of (–) (6,5) tube could potentially play a role, although to a lesser extent, in shielding a DNA-SWCNT complex from reacting with reactive dopant species.

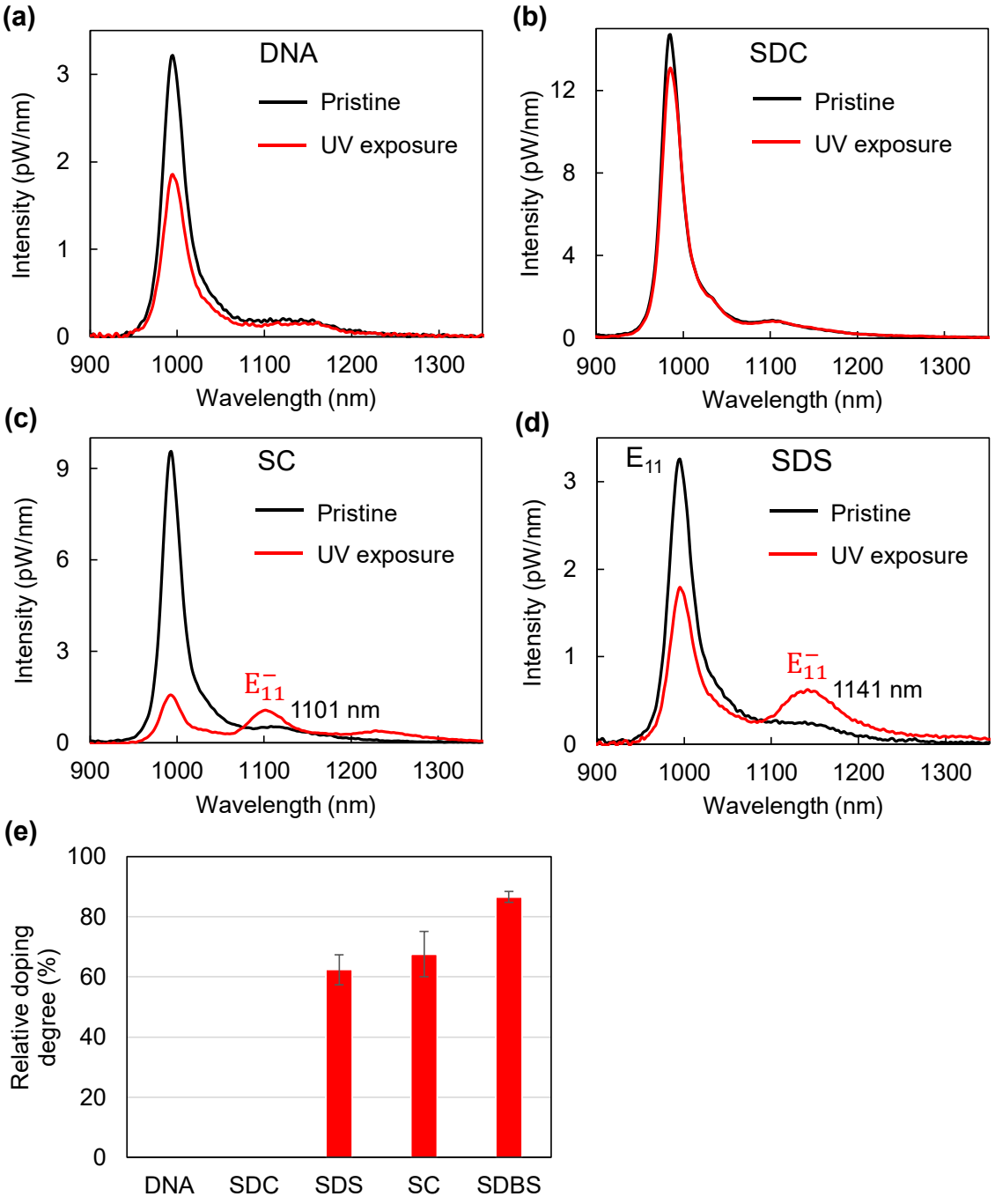

Figure 3. Fluorescence spectra of (–) (6,5) SWCNTs coated by different dispersing molecules including (a) the recognition DNA sequence TTA TAT TAT ATT, (b) SDC, (c) SC, and (d) SDS before (i.e., pristine) and after exposure to 254 nm UV light for 50 minutes. (e) Coating material-dependent relative doping degree, which is defined as the peak area ratio between the integrated fluorescence intensity of the defect-state E_{11}^{-} peaks (> 1050 nm) and the overall fluorescence intensity.

In comparison, (–) (6,5) nanotubes coated by SDBS, SDS, and SC have led to varying degrees of oxygen doping of SWCNTs as evidenced by the formation of defect-state E_{11}^{-} peaks with different optical properties (Figures 1a and 3c,d, Table S3). Specifically, SDBS exhibited the most efficient oxygen doping, with an emission intensity ratio I_{11}^{-}/I_{11} of 0.63 and an energy separation ΔE_{11} of 160 meV after photoreaction (Table S3). The oxygen doping of (–) (6,5) tubes complexed with SC and SDS is less efficient under the experimental condition used in this work, yielding I_{11}^{-}/I_{11} ratios of 0.09 and 0.18, as well as ΔE_{11} of 123 and 159 meV, respectively (Figures 3c,d and Table S3). Moreover, we obtained the relative doping degree from the peak area ratio between the PL intensity integrated over the defect-state E_{11}^{-} peak (> 1050 nm) and the total spectrally integrated PL intensity that includes the E_{11} peak after UV irradiation of SWCNT samples (Figure 3e and Figure S6).[22] Our results suggest that the oxygen doping of (–) (6,5) tube is strongly dependent on the coating material property. The surface coverage of nanotubes plays a certain role in oxygen doping, particularly for surfactant-coated tubes, as weaker surfactants such as SDS, SDBS, and SC are known to form sparse, disordered micellar structures on the SWCNT surface.[24,46,47] Additionally, UV irradiation of SDS- and SC-coated (–) (6,5) after oxygen removal showed no obvious E_{11}^{-} peak formation, further indicating the importance of dissolved oxygen in assisting the oxygen doping of SWCNTs (Figure S3).

Next, we explored further the effect of surface coverage of SWCNTs on oxygen doping by comparing the results of (±) (6,5) enantiomers wrapped by the same DNA recognition sequence

TTA TAT TAT ATT after UV (254 nm) irradiation (Figure 3a, Figure 4a, and Figure S8). In our prior work, the wrapping conformation of the same recognition DNA sequence on the two (6,5) enantiomers was found to be drastically different, leading to their separation in a polymer aqueous two-phase system.[23] Particularly, DNA-(–) (6,5) complex has higher surface coverage than that of DNA-(+) (6,5) as evidenced by its larger anhydrous density (density of the DNA-SWCNT complex without any contributions from the associated hydration shell) and being less susceptible to oxidation.[23] Similar to the outcome of DNA-(–) (6,5) complex, when DNA-(+) (6,5) was exposed to UV light, we observed no obvious formation of E_{11}^{-} emission peak, while the pristine E_{11} peak emission intensity decreased by 37 % (Figure 4a). The corresponding absorption spectrum of DNA-(+) (6,5) remains unchanged after UV irradiation (Figure S8a). After displacing DNA coatings of (+) (6,5) by SDBS, a new E_{11}^{-} emission peak appears around 1123 nm, accompanied by a decrease in the pristine E_{11} peak (Figure 4b). Furthermore, the emission intensity ratio I_{11}^{-}/I_{11} of SDBS-(+) (6,5) after photoreaction is 0.60 and the energy separation ΔE_{11} is 154 meV, similar to that of SDBS-(–) (6,5) complex (Table S3). The corresponding absorption spectrum of SDBS-(+) (6,5) showed nearly 64 % decrease in the E_{11} absorbance value after exposure to 254 nm UV light (Figure S8b). Direct comparison of fluorescence spectra of (±) (6,5) enantiomers coated by DNA and SDBS before and after UV (254 nm) irradiation is provided in Figure S9. These results highlight the significant role of the chemical compounds of coating materials as compared to the surface coverage of SWCNTs during the photochemical oxygen doping of nanotubes.

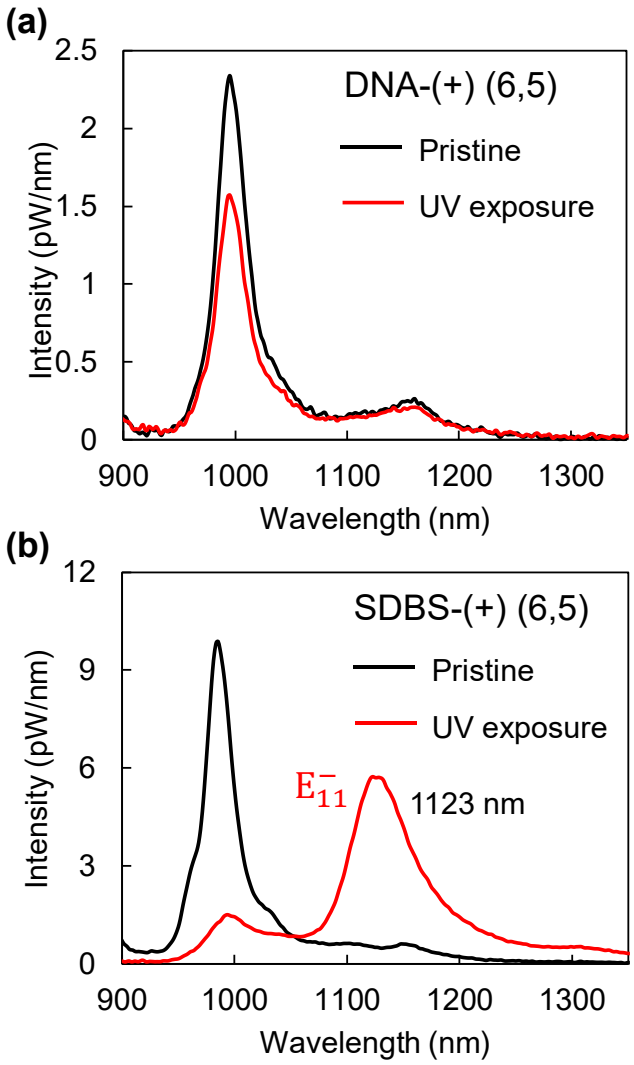

Figure 4. Fluorescence spectra of (a) DNA- and (b) SDBS-coated (+) (6,5) before (i.e., pristine) and after exposure to 254 nm UV light for 50 minutes.

CONCLUSIONS

In summary, we have demonstrated that the oxygen doping of SWCNTs is a readily occurring reaction in water with dissolved oxygen, where the reaction efficiency is strongly dependent on the UV light wavelength and the specific coating material on the nanotube surface. Particularly, DNA coatings react with ROS more competitively than that of SWCNTs, therefore acting as a protection layer around nanotubes against ROS. The surface coverage of SWCNTs by coating

materials plays a weaker role in the oxygen doping reaction as evidenced by the lack of photoreaction of the two (6,5) enantiomers that have drastically different surface coating structures formed from the same DNA sequence. Among the (6,5) samples coated by different molecules (DNA and surfactants), SDBS-(6,5) enantiomers showed the highest oxygen doping efficiency under exposure to 254 nm UV light, as seen by the formation of the defect-state E_{11}^{-} emission peak. These findings reveal important reaction mechanisms of oxygen-doped, pure-chirality SWCNTs with tunable optical properties. It also provides insights for controlling photochemical reactions of SWCNTs with other molecules and functional groups, by offering methods of circumventing the possible competing reaction of oxygen doping. Combined, our work contributes to the advancement of carbon nanotube chemistry in enabling novel applications, such as creating NIR fluorescent agents for biomedical sensing and imaging as well as providing new materials for optoelectronics development.

ASSOCIATED CONTENT

Supporting Information

The Supporting Information is available free of charge on the ACS Publications website.

Figures S1-S9 and Tables S1-S3.

AUTHOR INFORMATION

Corresponding Author

*Emails: g.ao@csuohio.edu

ORCID

Geyou Ao: 0000-0002-9932-3971

Present Address

F. X.: Department of Chemical Engineering, University of Michigan, 500 S State St Ann Arbor, MI 48109-1382

Notes

The authors declare no competing financial interest.

ACKNOWLEDGMENTS

We acknowledge support of National Science Foundation award (CBET-1917513). We would like to acknowledge Dr. Xue-Long Sun and Ka Keung Chan for help with oxygen removal experiments and useful discussions.

REFERENCES

(1) Iizumi, Y.; Yudasaka, M.; Kim, J.; Sakakita, H.; Takeuchi, T.; Okazaki, T. Oxygen-Doped Carbon Nanotubes for near-Infrared Fluorescent Labels and Imaging Probes. *Sci. Rep.* **2018**, *8*, 6272.

(2) Lin, C.-W.; Bachilo, S. M.; Zheng, Y.; Tsedev, U.; Huang, S.; Weisman, R. B.; Belcher, A. M. Creating Fluorescent Quantum Defects in Carbon Nanotubes Using Hypochlorite and Light. *Nat. Commun.* **2019**, *10*, 2874.

(3) Avouris, P.; Freitag, M.; Perebeinos, V. Carbon-Nanotube Photonics and Optoelectronics. *Nat. Photonics* **2008**, *2*, 341–350.

(4) He, X.; Hartmann, N. F.; Ma, X.; Kim, Y.; Ihly, R.; Blackburn, J. L.; Gao, W.; Kono, J.; Yomogida, Y.; Hirano, A., et al. Tunable Room-Temperature Single-Photon Emission at Telecom Wavelengths from sp^3 Defects in Carbon Nanotubes. *Nat. Photonics* **2017**, *11*, 577.

(5) Miyauchi, Y.; Iwamura, M.; Mouri, S.; Kawazoe, T.; Ohtsu, M.; Matsuda, K. Brightening of Excitons in Carbon Nanotubes on Dimensionality Modification. *Nat. Photonics* **2013**, *7*, 715–719.

(6) Ghosh, S.; Bachilo, S. M.; Simonette, R. A.; Beckingham, K. M.; Weisman, R. B. Oxygen Doping Modifies Near-Infrared Band Gaps in Fluorescent Single-Walled Carbon Nanotubes. *Science* **2010**, *330*, 1656–1659.

(7) Chen, J.; Dhall, R.; Hou, B.; Yang, S.; Wang, B.; Kang, D.; Cronin, S. B. Enhanced Photoluminescence in Air-Suspended Carbon Nanotubes by Oxygen Doping. *Appl. Phys. Lett.* **2016**, *109*, 153109.

(8) Ma, X.; Adamska, L.; Yamaguchi, H.; Yalcin, S. E.; Tretiak, S.; Doorn, S. K.; Htoon, H. Electronic Structure and Chemical Nature of Oxygen Dopant States in Carbon Nanotubes. *ACS Nano* **2014**, *8*, 10782–10789.
(9) Shiraishi, T.; Juhász, G.; Shiraki, T.; Akizuki, N.; Miyauchi, Y.; Matsuda, K.; Nakashima, N. Determination of Precise Redox Properties of Oxygen-Doped Single-Walled Carbon Nanotubes Based on *in situ* Photoluminescence Electrochemistry. *J. Phys. Chem. C* **2016**, *120*, 15632–15639.
(10) Piao, Y.; Meany, B.; Powell, L. R.; Valley, N.; Kwon, H.; Schatz, G. C.; Wang, Y. Brightening of Carbon Nanotube Photoluminescence through the Incorporation of sp^3 Defects. *Nat. Chem.* **2013**, *5*, 840–845.
(11) Powell, L. R.; Piao, Y.; Wang, Y. Optical Excitation of Carbon Nanotubes Drives Localized Diazonium Reactions. *J. Phys. Chem. Lett.* **2016**, *7*, 3690–3694.
(12) Berger, F. J.; Lüttgens, J.; Nowack, T.; Kutsch, T.; Lindenthal, S.; Kistner, L.; Müller, C. C.; Bongartz, L. M.; Lumsargis, V. A.; Zakharko, Y., et al. Brightening of Long, Polymer-Wrapped Carbon Nanotubes by sp^3 Functionalization in Organic Solvents. *ACS Nano* **2019**, *13*, 9259–9269.
(13) Maeda, Y.; Minami, S.; Takehana, Y.; Dang, J.-S.; Aota, S.; Matsuda, K.; Miyauchi, Y.; Yamada, M.; Suzuki, M.; Zhao, R.-S., et al. Tuning of the Photoluminescence and Up-Conversion Photoluminescence Properties of Single-Walled Carbon Nanotubes by Chemical Functionalization. *Nanoscale* **2016**, *8*, 16916–16921.
(14) Maeda, Y.; Konno, Y.; Yamada, M. Helicity Sorting and Optical Resolution of Functionalized Single-Walled Carbon Nanotubes and Their Optical Properties. *J. Phys. Chem. C* **2020**, *124*, 21886–21894.
(15) Iakoubovskii, K.; Minami, N.; Kim, Y.; Miyashita, K.; Kazaoui, S.; Nalini, B. Midgap Luminescence Centers in Single-Wall Carbon Nanotubes Created by Ultraviolet Illumination. *Appl. Phys. Lett.* **2006**, *89*, 173108.
(16) Shiraki, T.; Miyauchi, Y.; Matsuda, K.; Nakashima, N. Carbon Nanotube Photoluminescence Modulation by Local Chemical and Supramolecular Chemical Functionalization. *Acc. Chem. Res.* **2020**, *53*, 1846–1859.
(17) Hofmann, M. S.; Glückert, J. T.; Noé, J.; Bourjau, C.; Dehmel, R.; Högele, A. Bright, Long-Lived and Coherent Excitons in Carbon Nanotube Quantum Dots. *Nat. Nanotechnol.* **2013**, *8*, 502–505.
(18) Ma, X.; Hartmann, N. F.; Baldwin, J. K. S.; Doorn, S. K.; Htoon, H. Room-Temperature Single-Photon Generation from Solitary Dopants of Carbon Nanotubes. *Nat. Nanotechnol.* **2015**, *10*, 671–675.
(19) Crochet, J. J.; Duque, J. G.; Werner, J. H.; Lounis, B.; Cognet, L.; Doorn, S. K. Disorder Limited Exciton Transport in Colloidal Single-Wall Carbon Nanotubes. *Nano Lett.* **2012**, *12*, 5091–5096.
(20) He, X.; Velizhanin, K. A.; Bullard, G.; Bai, Y.; Olivier, J.-H.; Hartmann, N. F.; Gifford, B. J.; Kilina, S.; Tretiak, S.; Htoon, H., et al. Solvent- and Wavelength-Dependent Photoluminescence Relaxation Dynamics of Carbon Nanotube sp^3 Defect States. *ACS Nano* **2018**, *12*, 8060–8070.
(21) Alvarez, N. T.; Kittrell, C.; Schmidt, H. K.; Hauge, R. H.; Engel, P. S.; Tour, J. M. Selective Photochemical Functionalization of Surfactant-Dispersed Single Wall Carbon Nanotubes in Water. *J. Am. Chem. Soc.* **2008**, *130*, 14227–14233.

(22) Ma, X.; Baldwin, J. K. S.; Hartmann, N. F.; Doorn, S. K.; Htoon, H. Solid-State Approach for Fabrication of Photostable, Oxygen-Doped Carbon Nanotubes. *Adv. Funct. Mater.* **2015**, *25*, 6157–6164.
(23) Ao, G.; Streit, J. K.; Fagan, J. A.; Zheng, M. Differentiating Left- and Right-Handed Carbon Nanotubes by DNA. *J. Am. Chem. Soc.* **2016**, *138*, 16677–16685.
(24) Lin, S.; Blankschtein, D. Role of the Bile Salt Surfactant Sodium Cholate in Enhancing the Aqueous Dispersion Stability of Single-Walled Carbon Nanotubes: A Molecular Dynamics Simulation Study. *J. Phys. Chem. B* **2010**, *114*, 15616–15625.
(25) Haggenmueller, R.; Rahatekar, S. S.; Fagan, J. A.; Chun, J.; Becker, M. L.; Naik, R. R.; Krauss, T.; Carlson, L.; Kadla, J. F.; Trulove, P. C., et al. Comparison of the Quality of Aqueous Dispersions of Single Wall Carbon Nanotubes Using Surfactants and Biomolecules. *Langmuir* **2008**, *24*, 5070–5078.
(26) Fagan, J. A.; Zheng, M.; Rastogi, V.; Simpson, J. R.; Khripin, C. Y.; Silvera Batista, C. A.; Hight Walker, A. R. Analyzing Surfactant Structures on Length and Chirality Resolved (6,5) Single-Wall Carbon Nanotubes by Analytical Ultracentrifugation. *ACS Nano* **2013**, *7*, 3373–3387.
(27) Ao, G.; Zheng, M. Preparation and Separation of DNA-Wrapped Carbon Nanotubes. *Curr. Protoc. Chem, Biol.* **2015**, *7*, 43–51.
(28) Khripin, C. Y.; Arnold-Medabalimi, N.; Zheng, M. Molecular-Crowding-Induced Clustering of DNA-Wrapped Carbon Nanotubes for Facile Length Fractionation. *ACS Nano* **2011**, *5*, 8258–8266.
(29) Zheng, M.; Diner, B. A. Solution Redox Chemistry of Carbon Nanotubes. *J. Am. Chem. Soc.* **2004**, *126*, 15490–15494.
(30) Xhyliu, F.; Ao, G. Chirality-Pure Carbon Nanotubes Show Distinct Complexation with Recognition DNA Sequences. *Carbon* **2020**, *167*, 601–608.
(31) He, X.; Htoon, H.; Doorn, S. K.; Pernice, W. H. P.; Pyatkov, F.; Krupke, R.; Jeantet, A.; Chassagneux, Y.; Voisin, C. Carbon Nanotubes as Emerging Quantum-Light Sources. *Nat. Mater.* **2018**, *17*, 663–670.
(32) Iwamura, M.; Akizuki, N.; Miyauchi, Y.; Mouri, S.; Shaver, J.; Gao, Z.; Cognet, L.; Lounis, B.; Matsuda, K. Nonlinear Photoluminescence Spectroscopy of Carbon Nanotubes with Localized Exciton States. *ACS Nano* **2014**, *8*, 11254–11260.
(33) Zheng, Y.; Bachilo, S. M.; Weisman, R. B. Quenching of Single-Walled Carbon Nanotube Fluorescence by Dissolved Oxygen Reveals Selective Single-Stranded DNA Affinities. *J. Phys. Chem. Lett.* **2017**, *8*, 1952–1955.
(34) Briner, E. Photochemical Production of Ozone. In *OZONE CHEMISTRY AND TECHNOLOGY*; Advances in Chemistry; American Chemical Society: Washington, D.C., **1959**; Vol. 21, pp 1–6.
(35) Salvermoser, M.; Murnick, D. E.; Kogelschatz, U. Influence of Water Vapor on Photochemical Ozone Generation with Efficient 172 nm Xenon Excimer Lamps. *Ozone: Sci. Eng.* **2008**, *30*, 228–237.
(36) Farooq, Z.; Chestakov, D. A.; Yan, B.; Groenenboom, G. C.; van der Zande, W. J.; Parker, D. H. Photodissociation of Singlet Oxygen in the UV Region. *Phys. Chem. Chem. Phys.* **2014**, *16*, 3305-3316.
(37) Grujicic, M.; Cao, G.; Rao, A. M.; Tritt, T. M.; Nayak, S. UV-Light Enhanced Oxidation of Carbon Nanotubes. *Appl. Surf. Sci.* **2003**, *214*, 289–303.

(38) Tu, X.; Manohar, S.; Jagota, A.; Zheng, M. DNA Sequence Motifs for Structure-Specific Recognition and Separation of Carbon Nanotubes. *Nature* **2009**, *460*, 250–253.
(39) Roxbury, D.; Jagota, A.; Mittal, J. Structural Characteristics of Oligomeric DNA Strands Adsorbed onto Single-Walled Carbon Nanotubes. *J. Phys. Chem. B* **2013**, *117*, 132–140.
(40) Ito, K.; Inoue, S.; Hiraku, Y.; Kawanishi, S. Mechanism of Site-Specific DNA Damage Induced by Ozone. *Mutat. Res., Genet. Toxicol. Environ. Mutagen.* **2005**, *585*, 60–70.
(41) Sawadaishi, K.; Miura, K.; Ohtsuka, E.; Ueda, T.; Shinriki, N.; Ishizaki, K. Structure- and Sequence-Specificity of Ozone Degradation of Supercoiled Plasmid DNA. *Nucleic Acids Res.* **1986**, *14*, 1159–1169.
(42) Cadet, J.; Wagner, J. R. DNA Base Damage by Reactive Oxygen Species, Oxidizing Agents, and UV Radiation. *Cold Spring Harbor Perspect. Biol.* **2013**, *5*, a012559–a012559.
(43) Middleton, C. T.; de La Harpe, K.; Su, C.; Law, Y. K.; Crespo-Hernández, C. E.; Kohler, B. DNA Excited-State Dynamics: From Single Bases to the Double Helix. *Annu. Rev. Phys. Chem.* **2009**, *60*, 217–239.
(44) Ignatova, T.; Balaeff, A.; Blades, M.; Zheng, M.; Stoeckl, P.; Rotkin, S. V. Two-Color Spectroscopy of UV Excited ssDNA Complex with a Single-Wall Nanotube Photoluminescence Probe: Fast Relaxation by Nucleobase Autoionization Mechanism. *Nano Res.* **2016**, *9*, 571–583.
(45) Park, M.; Salem, D. P.; Parviz, D.; Gong, X.; Silmore, K. S.; Lew, T. T. S.; Khong, D. T.; Ang, M. C.-Y.; Kwak, S.-Y.; Chan-Park, M. B., et al. Measuring the Accessible Surface Area within the Nanoparticle Corona Using Molecular Probe Adsorption. *Nano Lett.* **2019**, *19*, 7712–7724.
(46) Duque, J. G.; Densmore, C. G.; Doorn, S. K. Saturation of Surfactant Structure at the Single-Walled Carbon Nanotube Surface. *J. Am. Chem. Soc.* **2010**, *132*, 16165–16175.
(47) Tummala, N. R.; Striolo, A. SDS Surfactants on Carbon Nanotubes: Aggregate Morphology. *ACS Nano* **2009**, *3*, 595–602.

TOC Graphic

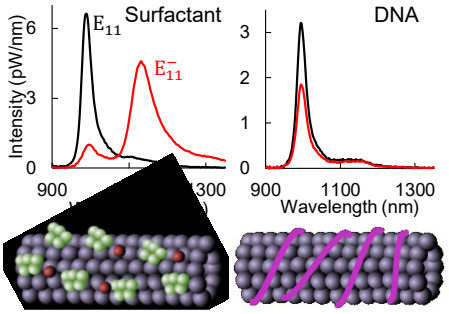
Surfactant
DNA
E_{11}
E_{11}^{-}
Intensity (pW/nm)
6
3
0
3
2
1
0
900
1100
1300
Wavelength (nm)